FCC Feedstocks/Bio-oils Co-processing: Towards understanding of phenolic compounds impact on Ni- and V-USY zeolites

R.T.J. Gerards
jacob.gerards@tecnico.ulisboa.pt

ABSTRACT: One option for the upgrading of bio-oils would be the co-feeding of liquefied biomass with conventional feedstock in the FCC process of existing petroleum refineries. The main difference between conventional petroleum feedstock and liquefied biomass is the higher oxygen amount of the latter, which has a deactivating effect on the FCC catalysts. The objective of this work is to understand the influence of oxygenated compounds on the catalytic properties of nickel and vanadium USHY zeolite present in the FCC catalysts. The transformation of n-heptane with and without guaiacol over USHY zeolite, with and without metal impregnation, was studied as a model reaction. It was seen that nickel has a higher deactivating effect on the catalyst activity, as compared to vanadium and USHY zeolite. This is consistent with a more pronounced increase in coke formation and decrease of Brønsted acid sites concentration upon nickel impregnation, as compared to vanadium. Guaiacol was less poisonous for nickel and vanadium (USHY > V-USHY > Ni-USHY), due to an increase of Lewis acid sites concentration upon metal impregnation. Guaiacol adsorbs preferentially onto Lewis acid sites, which result in relatively more Brønsted acid sites available for cracking reactions. Both nickel and vanadium induce an increase in hydrogen transfer and dehydrogenation reactions, which led to some changes in cracking products selectivity during pure n-heptane cracking. During guaiacol poisoning, no additional changes in product distribution were observed.

INTRODUCTION

An increasing demand for petroleum by emerging economies, decreasing petroleum resources and political and environmental concerns about fossil fuels are encouraging the search for new sources of liquid fuels. From the renewable energy sources currently available, biomass is the only renewable source of carbon that can be converted into liquid fuels and this is mainly done by pyrolysis and liquefaction. One option for the upgrading to biofuel would be the co-feeding of liquefied biomass with conventional feedstock in the FCC process of existing petroleum refineries. Existing modern facilities are able to handle a broad range of chemical compounds and thus little capital cost investment would be required [1-4].

The FCC process has proven to be a very flexible and robust process, as it can be used to convert a wide range of feedstocks into useful products. It is the most widely used process for the conversion of the heavy fractions of crude, such as heavy gas oil (HGO), vacuum gas oil (VGO) or residue feedstocks, into more valuable products, such as gasoline, middle distillate (LCO) and light olefins. The typical FCC equilibrium catalyst (ECAT) consists of several components, such as an inert matrix, active matrix, binder and dealuminated ultra-stable Y zeolite (US-Y). US-Y zeolite is the main active zeolite in the FCC catalyst for today's conventional FCC process, often in a rare-earth stabilized form. ZSM-5 is being used as additive to the FCC catalyst for the purpose of producing more propylene and olefins. Coke formation has a strong impact on catalyst performance by decreasing the conversion and modifying product selectivity, but it also has an important role in the heat balance of the FCC unit. [2, 5-8]

The main difference between conventional petroleum feedstock and liquefied biomass is the higher oxygen amount of the latter. Residues from biomass usually contain between 35 and 50 wt% oxygen, which is why bio-oils have some inconvenient properties for fuel applications; high corrosiveness, low miscibility with hydrocarbon fuels, higher tendency to form coke, thermal- and chemical instability, low heating value, etc. The major challenge in the conversion of biomass is the efficient removal of oxygen from hydrophilic biomass-derived feedstock to convert it into hydrophobic matter. In fact, because of the above-mentioned undesired properties, the direct addition of bio-oil to established processes like FCC is

not straightforward, thus creating the need for a previous HDO upgrading step. [1, 2, 5]

The amount of heavy feedstock that is used in refining operations has been increasing worldwide. These heavy feedstocks usually present a high amount of metals that are in part responsible for the FCC catalyst deactivation. The objective of this work is to understand the influence of nickel and vanadium on the deactivating effect of oxygenated compounds and catalytic properties of the FCC catalyst. Guaiacol, a phenolic compound, was used as representative of hydrotreated bio-oil. The deactivation phenomenon resulting from guaiacol poisoning and its influence on the activity, stability and product selectivity of the Y zeolite was studied in this thesis. A model compound study was conducted with CBV500, an US-Y zeolite, and n-heptane as representative of conventional hydrocarbon feedstock. The zeolite was impregnated with varying amount of nickel and vanadium to resemble the industrial composition of the ECAT mixture. The deactivating effect of guaiacol was studied with and without metal impregnation [5].

EXPERIMENTAL TECHNIQUES

Catalyst Preparation

The parent zeolite, ultra-stable Y zeolite CBV500, was impregnated with 0.5%, 1% and 2% nickel and vanadium to resemble the industrial composition of the ECAT mixture. Nickel and vanadium were introduced in the zeolite using dry impregnation, while cerium was introduced by an ion-exchange procedure. CBV500 was delivered by Zeolyst in the ammonium form, which makes it very suitable for post-synthesis modifications.

Dry (Incipient Wetness) Impregnation

For both nickel and vanadium three samples were prepared (0.5wt%, 1wt% and 2wt% metal in CBV500). Knowing the molecular weights of the metal salts $Ni(NO_3)_2 \cdot 6H_2O$ (nickel(II)nitrate hexahydrate) and NH_4VO_3 (ammonium vanadate) used for the procedure, it was possible to calculate the amount of salt needed for the impregnation. The metal salts were dissolved in an amount of H_2O that would fill the pores of the zeolite completely (0.95 mL/gr). For the ammonium vanadate it was necessary to heat up the solution to 50°C while stirring for the salt to dissolve. The solution with metal salt was dropped on the sample drop by drop, while stirring the sample manually with a glass rod. The saturated sample was aged (1h) before it was dried at 100°C (24h). The dried sample was calcined under the usual conditions used in the next section.

Calcination

The calcination was performed using the temperature profile shown below. First the sample was heated to 200°C (2°C/min). This step was used to let the water evaporate out of the zeolite structure, which could cause dealumination in a later stage at higher temperature. After a plateau at 200°C (1h) the sample was heated to 500°C (5°C/min) and the treatment was finished with a plateau at 500°C (6h). The procedure was performed under a steady air flow (60 mL/min/gr).

$$RT \xrightarrow{2^0C/min} 200^0C \xrightarrow{5^0C/min} 500^0C$$

Characterization of Catalyst

For the structural analysis of the fresh samples, X-ray diffraction (XRD) was performed on fresh CBV500 samples with and without impregnated metal, while UV-vis spectroscopy was only performed on fresh samples impregnated with nickel and vanadium. Fourier transform infrared spectrometry (FTIR) and nitrogen adsorption experiments were performed on all fresh and coked samples, as compared to elemental analysis, for determining carbon content in the zeolite, which was only performed with coked samples.

X-Ray Diffraction (XRD)

XRD measurements were performed to investigate the structure, phase composition and thermostability of the fresh catalyst samples with and without metal impregnation [9].

The structural characterization of all CBV500 samples was carried out with a D8 Advance diffractometer from Bruker (Bragg-Brentano geometry), using copper radiation (filtered with Ni slit) and equipped with a linear Lynxeye detector (192 silicon strip sensors). The powder XRD patterns were obtained from 5° to 70° (2θ), with a step size of 0.02° and a time per step of 2s.

UV-Vis Spectroscopy

UV-Vis diffuse reflectance spectroscopy (DRS UV-Vis) was performed to determine the electronic states of the present nickel and vanadium species [9]. The Kubelka-Munk function (equation 1) was used and presents a linear relation between analyte concentration and reflectance for this type of UV-Vis spectroscopy. R_∞ is the reflectance after scattering throughout the non-absorbing matrix of infinite depth [10].

$$f(R_\infty) = \frac{(1 - R_\infty)^2}{2R_\infty} \qquad \text{(Eq. 1)}$$

DRS UV–Vis spectra of powder samples were collected on a Varian Cary 5000 UV–Vis–NIR spectrophotometer, in the range 200-800 nm, with the

following spectroscopic parameters (spectral bandwidth of 4 nm, data interval of 1 nm and scan rate of 600 nm.min^{-1}). A Praying Mantis integration sphere accessory was used for this purpose. For all the samples, parent sample (starting zeolite, CBV500 material) was used as baseline reference. The UV-Vis DRS spectra obtained were then converted into F(R) (Kubelka-Munk function) spectra.

FTIR Spectroscopy

The Fourier Transform Infrared Spectrometric technique allows the analysis of fresh and coked zeolite acidity, which can be characterized by two methodologies:

- The hydroxyl (OH group) stretching vibration bands can be seen in the 3500 – 3800 cm^{-1} region of the spectrum. By analyzing these bands, it is possible to obtain information concerning Brønsted acid sites.
- The interaction of pyridine as probe molecule with the acid sites of the zeolite can be studied. For both Lewis and Brønsted acid sites this gives valuable information regarding the nature, concentration and strength of the acid sites.

Interaction of pyridine with the acid sites of the zeolites results in the appearance of some bands in the 1300 – 1700 cm^{-1} region that are characteristic for pyridine adsorbed on Lewis and Brønsted acid sites. The concentration of both Lewis and Brønsted acid sites can be determined through a modified Lambert-Beer law [5], by integrating the absorbance of the bands at 1455 and 1540 cm^{-1}, respectively. The extinction coefficients used for the Lewis and Brønsted acid site concentration were previously reported by M. Guisnet et al. [11]: 1.28 cm/μmol for the PyH^+ (pyridinium ions) and 1.15 cm/μmol for the PyL (pyridine coordinated to Lewis acids).

The measurements were done, using a Nexus Thermo Nicolet apparatus (64 scans and resolution of 4 cm^{-1}) equipped with a home-made vacuum cell, and using self-supported discs (5-10 mg cm^{-1}) and pyridine as the base probe molecule. After in-situ outgassing at 450°C (fresh samples) or 200°C (coked samples) for 3h under high vacuum (10^{-5} Torr), pyridine (99.99 %) was contacted with the sample at 150°C for 10 min and then evacuated at 150 °C (all the samples) and 250°C, 350°C and 450°C (fresh samples) for 30 min under high vacuum (10^{-5} Torr).

Nitrogen Adsorption Measurements

According to methodology by I. Graça [5], the fresh zeolite samples can be outgassed at 90°C (1h) followed by 350°C (3h) under vacuum. Coked zeolites are degassed at 110°C (1h) under vacuum. The pre-treatment of coked zeolite will be less severe, since removal of coke molecules that are deposited on the zeolite surface should be prevented [5].

Nitrogen adsorption measurements were carried out at -196°C on a Micrometrics ASAP 2010 apparatus. The low temperature favors the adsorption reaction and is therefore chosen on the boiling point of nitrogen [12]. Through analysis of the isotherm, t-plot and BJH adsorption and desorption, the type of pores (micro, meso), the volume of the micropores (V_{micro}) and the external surface area (S_{ext}) can be calculated.

The t-plot method, as proposed by Lippens and de Boer [13], compares the adsorption isotherm of a microporous material with the adsorption isotherm of a nonporous material with the same surface characteristics. The method allows the determination of micropore volume, surface area and to obtain information about the average pore size.

The film thickness on pore walls is assumed to be uniform, which makes it possible to obtain the statistical thickness (t) from the gas adsorption isotherms and a thickness equation can be constructed. In this experiment the thickness equation formula constructed by Harkins and Jura will be used. This equation represents nitrogen sorption at -196°C on nonporous adsorbents that contain oxidic surfaces, thus being representable for zeolitic materials. The experimental adsorption isotherm data is reconstructed as a t-curve through the conversion of p_0/p to statistical thickness by the thickness equation formula (equation 2).

$$t(\text{Å}) = \left[\frac{13.99}{0.034 - \log\left(\frac{P_0}{P}\right)}\right]^{\frac{1}{2}} \qquad \text{(Eq. 2)}$$

With equation 3 [14] the adsorbed volume can be calculated. V_f is the volume of the nitrogen in gaseous form (cm^3/g), 22414 is the molar volume (cm^3/mol, STP), M is the molar mass of the adsorbed nitrogen (g/mol) and ρ is the density of the liquid nitrogen (g/cm^3).

$$V_{ads} = \left(\frac{V_f * M}{22414 * \rho}\right) \qquad \text{(Eq. 3)}$$

Elemental Analysis

The carbon content on the zeolite was analyzed by LAIST (Laboratório de Análisis do IST) by using methodology M.M. 8.6 (A.E.)(2009-05-06). This analysis was done for all coked catalytic samples at 1.5 and 60min of TOS.

Catalytic Tests

A catalysts calcination pretreatment was performed by heating up to 200°C (5°C/min), followed by a plateau at this temperature (1h) and further heating to 450°C (5°C/min), followed by a plateau at 450°C (6h). The pretreatment is carried out under constant N_2 flow (60 cm^3/min) at atmospheric pressure. The fixed bed reactor is heated to the reaction temperature in a vertical oven. A thermocouple Cr/Ni will be placed close to the catalytic bed of the reactor to know the reaction temperature with high precision.

The reactor feed will be composed of 10 mol% n-heptane and 90 mol% N_2. Different amounts of guaiacol will be injected together with the n-heptane in the poisoning tests. The pure reactant flow will be controlled by a Methrom725 Dosimat, the mixture rate will be controlled by a KD Scientific perfusor and the N_2 flow is controlled (120cm^3/min) at atmospheric pressure and room temperature by a BROOK Instruments controller.

A conversion profile can be obtained by taking samples for different TOS (time-on-stream) values from 1.5 to 60 minutes, the first value being the time to get a stable reactant pressure in the reactor. A 10-position valve is used to capture these samples, before being analyzed through a GC chromatograph (SHIMADZU GC-14B) with a Plot Al_2O_3/KCl fused silica capillary column (50m). Nitrogen will be used as carrier gas and for detection a flame ionization detector will be used. At the detector the flowrate for hydrogen and air are 40 cm^3/min and 500 cm^3/min, respectively. In figure 1 the temperature profile of the GC column is illustrated. The data acquisition will be carried out by software that is commercialized by Shimadzu under the name Class VP. The same software is used to control the GC and the positioning of the 10-position valve.

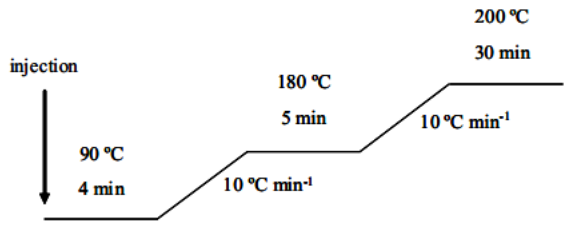

Figure 1 - GC column temperature profile for n-heptane [5]

Evaluation of the Catalyst Performance

From the results obtained from the GC with the flame ionization detector (FID), several performance metrics of the catalyst can be calculated. Since the FID is mass sensitive, the peak areas (A) from the GC are proportional to the mass concentration of the compounds in the product mixture and therefore also to the number of carbon atoms. Since the sensibility of the detector is dependent on the type of compounds that are analyzed, a response factor (F_R) should be given to each type of compound to obtain a corrected area (A_c). The response factor for n-heptane is close to 1, which makes it relatively simple to calculate the conversion, yield and selectivity of the n-heptane conversion [5].

Conversion on desorbed products (X (%)), yield (Y_i (wt%)) and selectivity (S_i (wt%)) for each product *i* can be calculated from the GC peak areas, as can be seen in equation 4-6. Coke is not accounted for in the peak areas, since coke molecules are trapped in the pores of the zeolite. This results in a smaller A_{total} in the calculations and therefor an underestimation for the conversion and overestimation for the yield and selectivity.

$$X\ (\%) = 100 - \frac{A_{reactant}}{A_{total}} \qquad \text{(Eq. 4)}$$

$$Y_i\ (wt\%) = \frac{A_i}{A_{total}} * 100 \qquad \text{(Eq. 5)}$$

$$S_i\ (wt\%) = \frac{A_i}{A_{tot.} - A_{reactant}} * 100 = \frac{Y_i}{X} * 100 \qquad \text{(Eq. 6)}$$

RESULTS & DISCUSSION

CBV500, a US-Y zeolite, was impregnated with varying amount of nickel and vanadium to resemble the metal deposition on the catalysts used in the FCC process during the cracking reaction of crude oil. The catalysts have been used in a model compound study in which the transformation of pure n-heptane and n-heptane with 1.2% guaiacol was under study. From the acquired data is was possible to evaluate the influence of nickel and vanadium on the deactivating effect of oxygenated compounds on the FCC catalysts.

Nickel and Vanadium impregnation

It was possible to determine the type of nickel and vanadium species after impregnation with UV-vis spectroscopy. Nickel species exist mainly as $Ni(H_2O)_6^{2+}$ species, which can be seen from bands 650nm and 720nm [15]. The band at 250nm is corresponding to NiO species (figure 2). In the case of vanadium, the species were partly tetrahedral coordinated species (240nm) that form vanadium monomer and oligomer and partly octahedral coordinated species (410nm) that form vanadium oligomers (figure 3) [16].

From XRD measurements, it was concluded that crystallinity did not change upon nickel or vanadium impregnation.

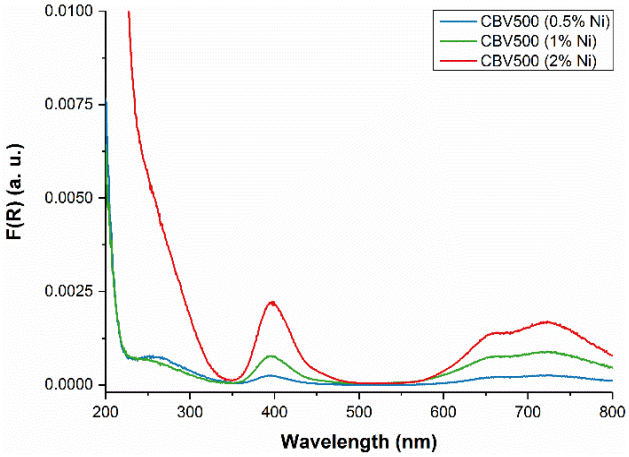

Figure 2 – Diffuse reflectance UV-vis spectra for nickel samples

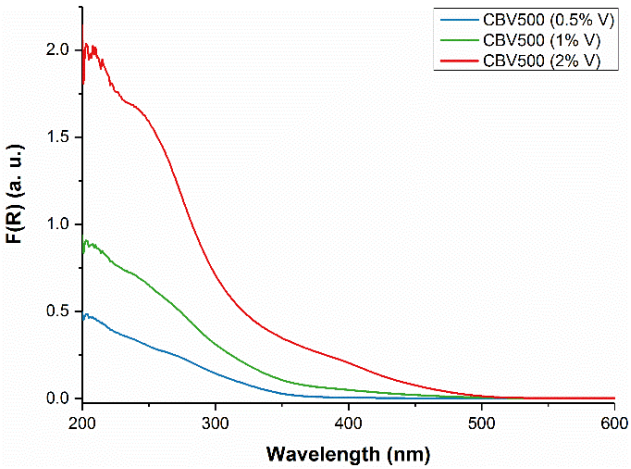

Figure 3 - Diffuse reflectance UV-vis spectra for vanadium samples

A small decrease in the mesoporous volume and external surface area can be seen for nickel and vanadium impregnated samples, which indicates that the metal is enriched on the external surface layer of the zeolite crystallite and to a minor extent in the mesopores of the zeolite (table 1). It was suggested that the presence of non-framework metallic cations in the pores of the zeolite, such as EFAL species, can complicate the migration of nickel particles [17]. A higher decrease observed for 2% vanadium samples could be the result of an increasing size of vanadium particle size, as compared to that of nickel particles.

Acid sites concentration was highly influenced by nickel, which resulted in a high increase of 54.5% in Lewis acid sites concentration and a decrease of 8.7% in Brønsted acid sites concentration, as compared to

Table 1 – Micro- and mesoporous volume and external surface area for fresh CBV500 with and without metal impregnation

	CBV500	0.5% Ni	2% Ni	0.5% V	2% V
V_{micro}	0.302	0.294	0.296	0.296	0.310
V_{meso}	0.078	0.075	0.072	0.074	0.064
S_{ext}	52.5	47.1	51.5	49.6	39.3

Table 2 – Brønsted- and Lewis acid sites concentration for fresh CBV500 with and without metal impregnation

CBV500	0.5% Ni	0.5% V
Lewis acid site concentration (mmol/gr)		
442	682	498
Brønsted acid site concentration (mmol/gr)		
816	744	796

the USHY zeolite without metal impregnation. In the case of vanadium impregnation, Lewis acid sites concentration increased about 12.6% and Brønsted acid sites concentration was similar (table 2). The significant increase in Lewis acid sites observed for nickel is due to the introduced nickel particles that can act as Lewis acid sites [18]. The decrease in Brønsted acidity can be the result of a reaction between NiO species and stronger Brønsted acid sites (equation 7) [17] or the replacements of protons by Ni^{2+} through ion exchange.

$$NiO + 2H^+ \rightarrow Ni^{2+} + H_2O \qquad \text{(Eq. 7)}$$

Pure n-heptane conversion - Activity

In the transformation of pure n-heptane over nickel and vanadium impregnated samples, a clear decrease in n-heptane conversion was observed for both metal catalysts, which is in agreement with conversion values obtained in previous research [19, 20]. For nickel the decrease was more pronounced with increasing nickel content and was observed for fresh and deactivated catalyst (1.5 – 60 min of TOS). For vanadium the decrease was also more pronounced with increasing metal content, but the decrease was lower than in the case of nickel impregnated samples and could only be seen for early times on stream (1.5 – 15 min of TOS) (figure 4).

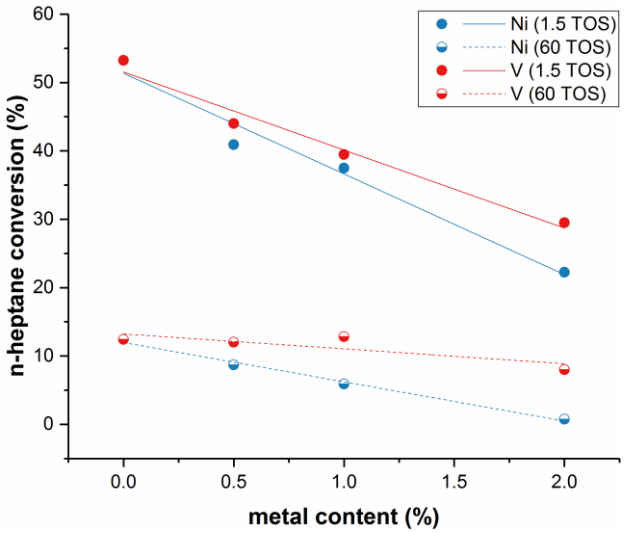

Figure 4 – Pure n-heptane conversion as a function of nickel and vanadium content for 1.5 and 60 min of TOS

Table 3 – Carbon content of coked catalysts after cracking of n-heptane with and without metal impregnation

			CBV500	0.5% Ni	2.0% Ni	0.5% V	2.0% V
TOS (min)	1.5	*pure n-heptane*	1.7%	1.8%	1.5%	1.8%	1.7%
		n-heptane + 1.2% guaiacol	1.6%	1.9%	3.5%	1.5%	1.9%
	60	*pure n-heptane*	9.4%	10.6%	15.7%	8.9%	8.7%
		n-heptane + 1.2% guaiacol	10.4%	14.1%	17.1%	10.8%	10.4%

Interaction of the metals with the Brønsted acid sites in the zeolite is assumed to be the reason for the decrease in initial activity. The main reason for the higher decrease for nickel samples, as compared so vanadium samples, could be the difference in deactivating effect of nickel and vanadium. Nickel has an inductive effect on the dehydrogenation reactions, with an increase in coke, and therefore a decrease in activity as the result.

In previous research it was seen that vanadium can have a detrimental effect as soon as its concentration is greater than 0.5% and steaming treatment is performed on the catalyst [20]. Similar results have not been observed in the current research, which signifies that introducing vanadium before steaming treatment induces a complete different result as compared to introducing vanadium in absence of a steaming treatment.

Carbon content for the pure n-heptane cracking reaction is illustrated in table 3. Higher carbon content was seen for deactivated nickel impregnated catalyst, which is consistent with the decrease in activity as compared to the reference sample. A higher increase in coke formation after nickel impregnation, as compared to vanadium, was seen in previous research [17, 19, 21]. Coke deposition was expected to increase also for vanadium impregnated samples [19, 21], but this is not seen in the current work. It is expected that this is due to a difference in catalyst preparation. In the research done by Escobar et al. [19] the metals in the catalysts were reduced, which led to an increase in coke formation. In the current work, the temperature does not exceed 500°C, thus reduction does not occur for vanadium impregnated samples. The increase in coke formation is due to (i) the increase in hydrogen transfer reaction that is favored by impregnated metals [22] and (ii) reduced nickel that has a higher tendency to form coke as compared to cationic nickel species [19]. Nickel can be reduced with temperatures below 500°C [17], thus nickel species could have been reduced in the current work.

During the cracking reaction only nickel impregnated catalysts showed a relatively high decrease of Lewis acid sites (-40%) as compared to the reference (-19%) and vanadium impregnated samples (-24%) (table 5). A possible explanation would be the interaction of nickel hydroxyls with coke molecules, which makes them unable to adsorb pyridine.

A decrease in microporous volume can be seen for all samples while mesoporous volume and external surface area did not change significantly (table 4). From the data it can be concluded that coke is mostly located in the micropores of the zeolite for all studied catalysts.

Table 4 – Micro- and mesoporous volumes and external surface areas for fresh and coked CBV500 with and without metal impregnation

	CBV 500	0.5% Ni	2% Ni	0.5% V	2% V
			V_{micro}		
fresh	0.302	0.294	0.296	0.296	0.310
n-heptane	0.264	0.248	0.266	0.270	0.260
nhp + guaiacol	0.270	0.245	0.242	0.272	0.212
			V_{meso}		
fresh	0.078	0.075	0.072	0.074	0.064
n-heptane	0.081	0.071	0.072	0.073	0.060
nhp + guaiacol	0.080	0.072	0.071	0.075	0.066
			S_{ext}		
fresh	52.5	47.1	51.5	49.6	39.3
n-heptane	55.4	41.4	51.6	47.8	42.8
nhp + guaiacol	54.3	43.5	50.5	51.4	45.6

Pure n-heptane conversion - Products selectivity

It can be seen in table 6 that the aromatics selectivity increases slightly when CBV500 is impregnated with nickel or vanadium, which could be the result of an increase in hydrogen transfer reactions with the introduction of metal species. Less change is detected for nickel impregnated sample, as compared to vanadium. This is in agreement with previous research, in which vanadium affects essentially the activity of the impregnated catalyst but not the selectivity [20].

From the detailed products selectivities (table 7) an increase in C_1, C_2 and n-C_4 selectivity can be observed for nickel impregnated sample. This is the

Table 5 – Brønsted- and Lewis acid sites concentration for fresh and coked CBV500 with and without metal impregnation

	CBV500	0.5% Ni	0.5% V
	Lewis acid site concentration (mmol/gr)		
fresh	442	682	498
nhp	335	407	404
nhp + guaiacol	301	456	420
	Brønsted acid site concentration (mmol/gr)		
fresh	816	744	796
nhp	672	624	615
nhp + guaiacol	631	731	695

Table 6 – Product group selectivity for cracking of n-heptane with and without nickel or vanadium impregnation

	Pure n-heptane		N-heptane + 1.2% guaiacol	
Nickel content (%)	*Cracking products (C1-C6) selectivity (%)*	*Aromatics selectivity (%)*	*Cracking products (C1-C6) selectivity (%)*	*Aromatics selectivity (%)*
0	96.0	4.0	96.3	3.7
0.5	94.4	5.6	95.3	4.7
2	92.4	7.6	91.3	8.7
Vanadium content (%)	*Cracking products (C1-C6) selectivity (%)*	*Aromatics selectivity (%)*	*Cracking products (C1-C6) selectivity (%)*	*Aromatics selectivity (%)*
0	96.0	4.0	96.3	3.7
0.5	94.4	5.6	95.9	4.1
2	94.8	5.2	94.8	5.2

result of increasing importance of the protolytic cracking mechanism. The increase in C_1, C_2 and aromatics with increasing nickel content is in line with expectation. Nickel deposited on the cracking catalyst causes nonselective cracking, which leads to increase coke and hydrogen production [17].

For vanadium no significant change was detected in the products selectivities.

A clear decrease in iso-paraffin / n-paraffin ratio was seen for both metals. Two situations could induce the decrease in iso-paraffin / n-paraffin ratio: i) The importance of the β-scission mechanism decreases relatively to the protolytic cracking reactions or ii) there are more spatial constraints to the branched molecules diffusion. Since C_1 and C_2 selectivity increases with increasing nickel content the first option is very plausible for nickel impregnated samples. With the increased coke production observed there is also a decrease in space available for diffusion, which would induce spatial constraints for iso-paraffins. It is plausible that both explanations are relevant for nickel impregnated samples, while only the latter is relevant for vanadium impregnated samples.

Guaiacol poisoning - Activity

For both nickel and vanadium impregnated samples there is a decrease in n-heptane conversion when guaiacol is added to the reaction mixture, as compared to pure n-heptane conversion (figure 5). For vanadium the decrease in n-heptane conversion is lower than for nickel impregnated samples. This is probably due to the higher decrease in Brønsted acid sites in case of nickel impregnation (table 2).

Residual activity for both nickel and vanadium impregnated samples can be seen in figure 6. From the positive slope in the residual activity graphs it can be seen that the deactivation is lower with increasing metal content. From this it can be concluded that guaiacol has a less poisonous effect with increasing metal content.

The effect that is described above is more pronounced for nickel than for vanadium and that is consistent with the higher increase in Lewis acid sites upon nickel impregnation (table 2). Additional Lewis

Table 7 – Detailed product selectivities for cracking of n-heptane with and without nickel or vanadium impregnation

	Pure n-heptane					N-heptane + 1.2% guaiacol				
	Ref.	*Nickel*		*Vanadium*		*Ref.*	*Nickel*		*Vanadium*	
		0.5%	*2%*	*0.5%*	*2%*		*0.5%*	*2%*	*0.5%*	*2%*
C1	0.1	0.3	2.8	0.2	0.3	0.1	0.3	2.1	0.2	0.4
C2	1.4	1.6	4.5	1.4	1.2	1.5	1.7	4.0	1.5	1.7
C3	28.4	26.2	28.7	27.2	27.3	28.5	27.3	26.9	27.6	29.8
C3=	10.6	12.2	9.5	11.7	10.5	10.6	11.5	10.2	11.5	10.5
i-C4	34.4	31.3	28.2	32.2	32.8	34.7	33.2	28.9	33.1	33.7
n-C4	9.5	10.7	10.5	10.3	10.7	9.6	9.9	10.1	10.3	11.4
C4=	5.0	5.8	4.2	5.4	4.9	4.7	5.1	4.4	5.2	4.6
i-C5	4.2	4.0	2.8	4.0	4.0	4.2	3.9	3.0	4.0	3.9
n-C5	1.1	1.0	0.8	1.0	0.9	1.0	1.0	0.8	0.9	0.9
C5=	0.5	0.6	0.3	0.5	0.3	0.5	0.5	0.3	0.5	0.4
C6	0.7	0.6	0.1	0.6	0.6	0.6	0.7	0.4	0.7	0.5
C6=	0.1	0.2	0.1	0.1	0.1	0.1	0.2	0.1	0.2	0.1
toluene	2.2	2.6	4.6	2.9	2.3	2.0	2.6	5.1	2.2	2.6
m,p-xylene	1.5	2.4	2.4	2.2	1.7	1.4	1.8	2.9	1.6	1.9
o-xylene	0.3	0.5	0.6	0.4	1.1	0.3	0.4	0.7	0.4	0.9

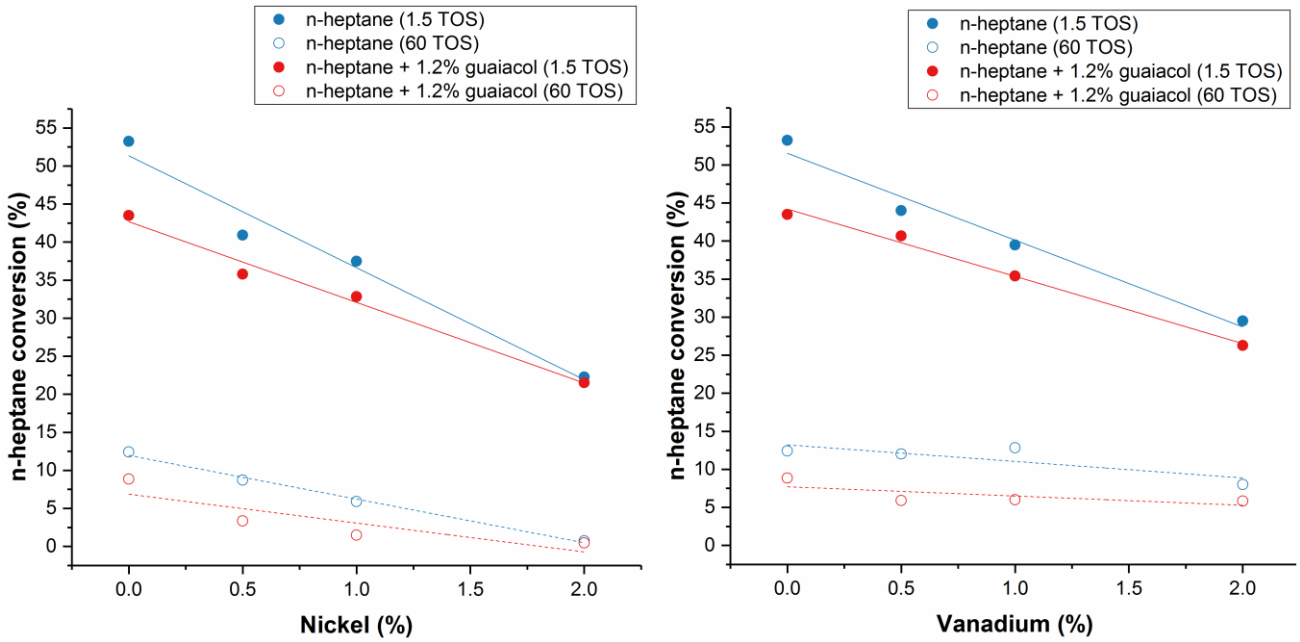

Figure 5 – n-heptane conversion with and without guaiacol versus metal content for nickel (left) and vanadium (right) impregnated CBV500

acid sites (Ni-USHY > V-USHY > USHY) can protect the Brønsted acid sites from the poisoning of guaiacol that bonds to both Lewis and Brønsted acid sites. This is consistent with the decrease in Brønsted acid sites after the cracking reaction in presence of guaiacol. The decrease in Brønsted acid site concentration is 22.6%, 12.7% and 1.74% for reference, vanadium impregnated and nickel impregnated sample, respectively.

Carbon content is higher at 1.5 and 60 min of TOS for nickel as compared to the reference and vanadium impregnated samples (table 3). Especially high coke deposition for nickel samples at 60 min of TOS is the reason for the very low activity of coked nickel impregnated catalyst. From the nitrogen adsorption data after cracking in presence in guaiacol (table 4), a decrease in microporous volume can be seen and is consistent with an increase in coke deposition. Mesoporous volume and external surface area show no significant change. For the cracking reaction in presence of guaiacol, the coke is therefore mostly located in the micropores of the zeolites.

Guaiacol poisoning – Products selectivity

A slight decrease in aromatics selectivity is seen in the case of guaiacol poisoning for both metals (table 6). A possible explanation would be the binding of guaiacol to metal species, thus reducing the importance of hydrogen transfer and dehydrogenation reaction associated with the impregnated metal catalysts.

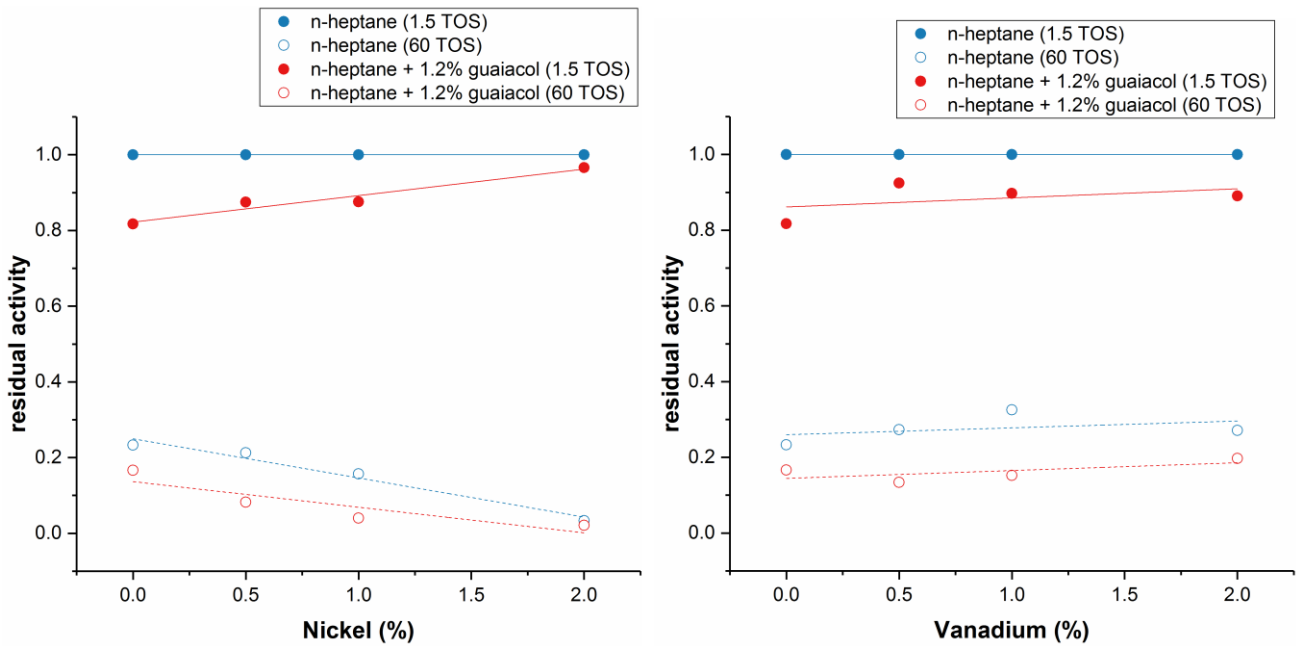

Figure 6 - Residual activities for cracking of n-heptane with and without guaiacol versus metal content for nickel (left) and vanadium (right) impregnated CBV500

Compared to pure n-heptane cracking, no very significant changes can be detected in the detailed product distribution when introducing guaiacol.

As opposed to the reference and vanadium impregnated samples, a significant increase in iso-paraffin / n-paraffin ratio was seen for nickel impregnated catalyst when introducing guaiacol to the reaction mixture. This is consistent with the increase in coke deposition (table 3) and Lewis acid sites concentration (table 2) upon nickel impregnation, which results in more potential places for guaiacol to replace coke molecules. This leads to a reduction in spatial constraints, and thus an increase in iso-paraffin selectivity.

CONCLUSION

Nickel and Vanadium impregnation

It was possible to determine the type of nickel and vanadium species after impregnation with UV-vis spectroscopy. Nickel species exist mainly as $Ni(H_2O)_6^{2+}$ and NiO species. In the case of vanadium, the species were partly tetrahedral coordinated species that form vanadium monomer and oligomer and partly octahedral coordinated species that form vanadium oligomers.

It was seen that the metal is enriched on the external surface layer of the zeolite crystallite and to a minor extent in the mesopores of the zeolite. An increase in Lewis acid sites was observed for both metals, while Brønsted only decreased in case of nickel impregnation. An increase in Lewis acid sites is due to the introduced metal particles that can act as Lewis acid sites. The decrease in Brønsted acidity can be the result of a reaction between nickel species and stronger Brønsted acid sites or the replacements of protons by Ni^{2+} through ion exchange.

Pure n-heptane conversion - Activity

In the transformation of pure n-heptane over nickel and vanadium impregnated samples, a clear decrease in n-heptane conversion was observed for both metal catalysts. Interaction of the metals with the Brønsted acid sites in the zeolite is assumed to be the reason for the decrease in initial activity. Higher carbon content was seen for deactivated nickel impregnated catalyst, which is consistent with the decrease in activity as compared to the reference sample. During the cracking reaction only nickel impregnated catalysts showed a relatively high decrease of Lewis acid sites, likely due to an interaction of nickel hydroxyls with coke molecules. It was concluded that coke is mostly located in the micropores of the zeolite for all studied catalysts.

Pure n-heptane conversion - Products selectivity

It can be seen that the aromatics selectivity increases slightly when CBV500 is impregnated with nickel or vanadium, which could be the result of an increase in hydrogen transfer reactions with the introduction of metal species. From the detailed products selectivities, an increasing importance of the protolytic cracking mechanism was observed in the case of nickel impregnated catalyst. For vanadium no significant change was detected in the products selectivities.

Guaiacol poisoning - Activity

For both nickel and vanadium impregnated samples there is a decrease in n-heptane conversion when guaiacol is added to the reaction mixture, as compared to pure n-heptane conversion. However, from the residual activity is can be seen that the deactivation is lower with increasing metal content. From this it can be concluded that guaiacol has a less poisonous effect with increasing metal content. This effect is more pronounced for nickel than for vanadium and that is consistent with the higher increase in Lewis acid sites for nickel.

Guaiacol poisoning – Products selectivity

A slight decrease in aromatics selectivity is seen in the case of guaiacol poisoning for both metals, likely due to a decreasing importance of hydrogen transfer and dehydrogenation reactions when guaiacol bonds to metal particles. Compared to pure n-heptane cracking, no very significant changes can be detected in the detailed product distribution when introducing guaiacol. An increase in iso-paraffin / n-paraffin ratio was seen for nickel impregnated catalyst when introducing guaiacol to the reaction mixture. This is consistent with the increase in coke deposition and Lewis acid sites concentration upon nickel impregnation, which results in more potential places for guaiacol to replace coke molecules.

Future research

- For vanadium impregnated samples the decrease in activity observed was low, as compared to results obtained in previous research efforts. This is mostly due to the fact that the deactivating effect of vanadium is more pronounced after steaming treatment, which could also have an influence on the product distribution. For that reason it would be interesting to perform a streaming treatment after impregnation to have a better resemblance of the industrial FCC catalyst.
- It was observed that guaiacol is adsorbed on both Lewis and Brønsted acid sites. Lewis acid sites can protect Brønsted acid sites from guaiacol poisoning. Alumina possesses only Lewis acid sites and could therefore give protection to the cracking catalyst. It would be interesting to mix HY zeolite with alumina to observe if a decrease in deactivating effect of guaiacol can be observed.

- RE introduced in the cracking zeolite can protect the catalyst from deactivation by vanadium through a process called *metal trapping*. It would be of interest to study the influence of solely RE content or together with vanadium.

[1] Graça, Inês, et al. "Bio-oils Upgrading for Second Generation Biofuels." Industrial & Engineering Chemistry Research, vol. 52, no. 1, 2013, pp. 275-287.

[2] Corma, A., et al. "Processing biomass-derived oxygenates in the oil refinery: Catalytic cracking (FCC) reaction pathways and role of catalyst." Journal of Catalysis, vol. 247, no. 2, 2007, pp. 307-327.

[3] Zacher, Alan H., et al. "A review and perspective of recent bio-oil hydrotreating research." Green Chem, vol. 16, no. 2, 2014, pp. 491-515.

[4] Talmadge, Michael S., et al. "A perspective on oxygenated species in the refinery integration of pyrolysis oil." Green Chem, vol. 16, no. 2, 2014, pp. 407-453.

[5] Graça, Inês. "Influence of Oxygenated Compounds on the Properties of FCC Catalysts." 2010. Instituto Superior Técnico, PhD Dissertation.

[6] Vogt, E. T., and B. M. Weckhuysen. "ChemInform Abstract: Fluid Catalytic Cracking: Recent Developments on the Grand Old Lady of Zeolite Catalysis." ChemInform, vol. 46, no. 48, 2015.

[7] Akah, Aaron. "Application of rare earths in fluid catalytic cracking: A review." Journal of Rare Earths, vol. 35, no. 10, 2017, pp. 941-956.

[8] H.S. Cerqueira, G. Caeiro, L. Costa, F. Ramôa Ribeiro. "Deactivation of FCC catalysts." Journal of Molecular Catalysis A: Chemical, vol. 292, 1 July 2008, pp. 1-13.

[9] Petranovskii, V., et al. "Formation of catalytically active copper and nickel nanoparticles in natural zeolites." Zeolites and related materials: Trends, targets and challenges, Proceedings of the 4th International FEZA Conference, 2008, pp. 513-516.

[10] Steward, Genevieve C. "Diffuse Reflectance Spectroscopy for the Characterization of Calcareous Glacial Till Soils from North Central Montana." 2006. Montana State U, MS thesis.

[11] Morin, S., et al. "Influence of the framework composition of commerical HFAU zeolites on their activity and selectivity in m-xylene transformation." Applied Catalysis A: General, vol. 166, no. 2, 1998, pp. 281-292.

[12] Trunschke, Annette. "Surface area and pore size determination." Modern Methods in Heterogeneous Catalysis Research, 1 Nov. 2013, Presentation.

[13] De Boer J. H. Lippens B.C, Linsen B.G., Broeckhoff J.C.P., van den Heuvel A., and Onsinga T.V., (1966), J. Colloid Interf. Sci. 21

[14] Leofanti, G., et al. "Surface area and pore texture of catalysts." Catalysis Today, vol. 41, no. 1-3, 1998, pp. 207-219.

[15] Petranovskii, V., et al. "Formation of catalytically active copper and nickel nanoparticles in natural zeolites." Zeolites and related materials: Trends, targets and challenges, Proceedings of the 4th International FEZA Conference, 2008, pp. 513-516.

[16] Venkatathri, N. "Structural and Catalytic Properties of a Novel Vanadium Containing Solid Core Mesoporous Shell Silica Catalysts for Gas Phase Oxidation Reaction." The Open Catalysis Journal, vol. 5, no. 1, 2012, pp. 14-20.

[17] LongXiang, T., et al. "Characteristics of the poisoning effect of nickel deposited on USY zeolite." Applied Catalysis A: General, vol. 91, no. 2, 1992, pp. 67-80.

[18] Wong, Syieluing, et al. "Catalytic Cracking of LDPE Dissolved in Benzene Using Nickel-Impregnated Zeolites." Industrial & Engineering Chemistry Research, vol. 55, no. 9, 2016, pp. 2543-2555.

[19] Escobar, Alyne S., et al. "Role of nickel and vanadium over USY and RE-USY coke formation." Applied Catalysis A: General, vol. 315, 2006, pp. 68-73.

[20] Torrealba, M., et al. "Influence of vanadium on the physicochemical and catalytic properties of USHY zeolite and FCC catalyst." Applied Catalysis A: General, vol. 90, no. 1, 1992, pp. 35-49.

[21] Yang, Shien-Jen, et al. "The interaction of vanadium and nickel in USY zeolite." Zeolites, vol. 15, no. 1, 1995, pp. 77-82.

[22] Cumming, K. A., and B. W. Wojciechowski. "Hydrogen Transfer, Coke Formation, and Catalyst Decay and Their Role in the Chain Mechanism of Catalytic Cracking." Catalysis Reviews, vol. 38, no. 1, 1996, pp. 101-157.